기계적 및 항균특성이 강화된 열가소성 Poly(lactic acid)와 4기화된 Chitosan-Saponite 나노복합체에 관한 연구

Xi Xi, Weijun Zhen[†], Shengzhen Bian*, and Wentao Wang

Key Laboratory of Oil and Gas Fine Chemicals, Ministry of Education and
Xinjiang Uygur Autonomous Region, Xinjiang University
*Xinjiang Institute of Light Industry Technology
(2014년 12월 18일 접수, 2015년 2월 16일 수정, 2015년 2월 18일 채택)

Enhancement of Mechanical and Antimicrobial Properties of Thermoplastic Poly(lactic acid)/Quaternized Chitosan-Saponite Nanocomposites

Xi Xi, Weijun Zhen[†], Shengzhen Bian*, and Wentao Wang

*Key Laboratory of Oil and Gas Fine Chemicals, Ministry of Education and Xinjiang Uygur Autonomous Region,
Xinjiang University, Urumqi 830046, P. R. China*
*Xinjiang Institute of Light Industry Technology, Urumqi 830021, P. R. China
(Received December 18, 2014; Revised February 16, 2015; Accepted February 18, 2015)

Abstract: Water-soluble *N*-(2-hydroxyl) propyl-3-trimethyl ammonium chitosan chloride (HTCC) was prepared with 2, 3-epoxypropyl trimethyl ammonium chloride grafting to the amino groups of chitosan. Then, chitosan quaternary ammonium intercalated saponite (HTCC-saponite) was synthesized with HTCC and saponite by ultrasonication intercalation. Compared with chitosan, HTCC had a good antibacterial effect. Thermoplastic poly(lactic acid) (PLA)/HTCC-saponite nanocomposites were prepared with HTCC-saponite and PLA by melt intercalation. Fourier transform infrared (FTIR) and nuclear magnetic resonance (^{1}H NMR) showed that HTCC was successfully synthesized by a modified method of two-step reaction. Moreover, X-ray diffraction (XRD) and scanning electron microscope (SEM) also showed that saponite was intercalated or nearly exfoliated by HTCC. It was shown the mechanical properties of PLA/HTCC-saponite nanocomposites attained the optimum when the content of HTCC-saponite was 1 phr. The studies of thermal stability, crystallization and rheological behavior of PLA/HTCC-saponite nanocomposites demonstrated that PLA/HTCC-saponite nanocomposites exhibited high performance compared with PLA.

Keywords: chitosan quaternary ammonium, melt intercalation, poly(lactic acid), saponite, nanocomposites.

Introduction

With the development of science and technology, people improved the environmental awareness, so the renewable resources of "green" materials would be relied on. They would not involve the use of toxic or noxious components in their manufacture, and could naturally take place degradation with composting or could be easily recycled.[1,2] In recent years, scientific and industrial interest in poly(lactic acid) (PLA) derived from a renewable agricultural resource is increasing due to easy degradation by simple hydrolysis. This latter fea-ture makes PLA be friendly to the environment. PLA has good biocompatibility, thus being a promising polymer for various end-use applications. Furthermore, the properties of PLA can be modified in a controlled manner by changing its stereo-chemical structure (in the polymerization stage, i.e., with a mixture of the L or D isomers) and/or by blending it with selected polymers or filling it with inorganic microparticles or nanoparticles.[3] So PLA is undoubtedly one of the most promising candidates for further developments. However, some drawbacks such as brittleness, poor toughness and thermal stability, low degree of crystallinity, slow crystallization rate and so on, all of these limited its use in practical processing, especially in the film extrusion industry.[4,5] Therefore, it is very important to improve the crystallization rate and properties of

[†]To whom correspondence should be addressed.
 E-mail: zhenweijun6900@163.com

PLA for developing the application of PLA composite materials by modification[6] and blending.[7] Some studies found[8-10] that clay particles not only performed an excellent heterogeneous nucleation effect in PLA matrix, but also increased the crystallization rate of PLA and promoted the cold crystallization process at low temperatures.

Saponite is a rare layered silicate mineral from Xinjiang of China which has trioctahedron structure and excellent properties.[11] Moreover, saponite has high ratio surface area and high heat stability.[12] For compatibility reasons, saponite is hydrophilic by nature and polymers mostly are hydrophobic, so saponite needs to be modified suitably with organic species in order to use it in the preparation of polymer based nanocomposites.[13]

Chitosan (CTS), the deacetylated derivative of chitin, as a natural renewable resource,[14] which has a number of unique properties such as antimicrobial activity, nontoxicity and biodegradability, which attract scientific and industrial interest in the fields of biotechnology, pharmaceutics, wastewater treatment, food science and textiles.[15,16] Despite all these advantages, but due to the fact that CTS contains a large number of amino and hydroxyl groups, and its intramolecular hydrogen bonding interaction is very strong so that CTS lacks of solubility in water and can only be dissolved in above pH 6.5,[17] which limits its application. Therefore, it is extremely necessary to prepare functional CTS to increase its solubility in water and broaden its applications.[18,19] Introduction of quaternary ammonium salts onto the chitosan backbone will be one of the best methods to enhance antimicrobial activity as well as the water solubility of chitosan over the entire pH range. In this work, N-(2-hydroxyl) propyl-3-trimethyl ammonium chitosan chloride (HTCC) was prepared by a relatively easy chemical reaction of CTS and glycidyl-trimethyl-ammonium chloride. HTCC has good solubility in water and antimicrobial properties, meanwhile without destroying the unique excellent performance of CTS. HTCC can inhibit the growth of bacteria in acid, water and base solution while CTS only shows antibacterial activity in acid solution.[20] Besides, HTCC is potential to be used as an absorption enhancer across intestinal epithelial due to its enhancement of mucoadhesion and permeability. It is well suitable for biomedical application.[21]

In the work, HTCC with antimicrobial function was employed as organo-modifier to improve the comprehensive performance of saponite. Moreover, thermoplastic PLA/HTCC-saponite nanocomposites were prepared by melt intercalation. To the best of our knowledge, there were few literatures on thermoplastic PLA/HTCC-saponite nanocomposites. Consequently, HTCC-saponite will endow PLA materials with properties of HTCC, and improve the crystallization properties and other performance of PLA. Furthermore, the effects of HTCC-saponite on properties and structure of PLA were investigated, respectively.

Experimental

Materials. PLA (L-form, injection grade, M_v=80000) was purchased from Shenzhen Guanghuaweiye Industrial Co., China. Nature saponite powder (cationic exchange capacity of about 75 mmol per 100 g, and mean grain size was about 60-70 μm) was purchased from Xinjiang Tuogema Colloid Co., China. Acetyl tributyl citrate (ATBC) (industrial grade, plasticizer) was provided by Changzhou Tianzheng Chemical Technology Co., China. Chitosan was purchased from Kelong Biochemical Co., Ltd. of China (The deacetylation degree was 85%, M_w=100000-300000). All other reagent grade chemicals such as hydrochloric acid, sodium hydroxide, ethanol, acetone and acetic acid were purchased from Qingdao Chemical Co, China.

Bacillus subtilis and *E. coli (Escherichia coli)* were provided by The Agronomy Soil Microbiology Teaching and Research Section of Xinjiang Agricultural University, *Aspergillus (Aspergillus SPP)* and *Penicillium (Penicillium SPP)* were provided by College of Food and Drug of Xinjiang Agricultural University.

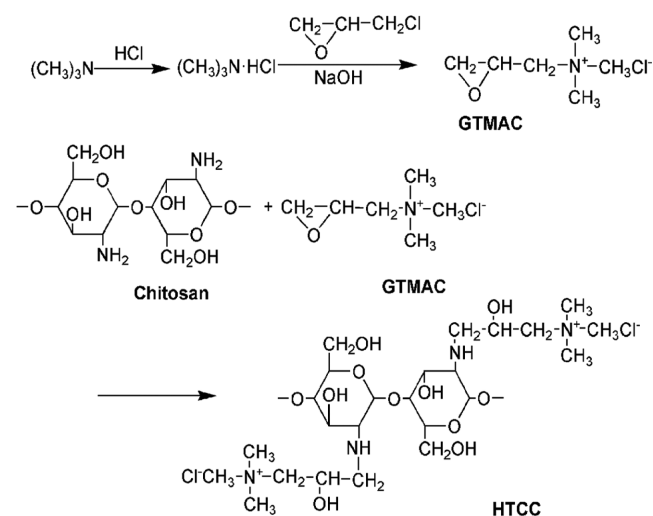**Preparation of HTCC-saponite.** The HTCC was prepared by a modified method of two-step reaction as shown in Figure

Figure 1. Synthesis scheme of HTCC.

1.[22] The delamination of saponite was performed via the combination of intercalation and ultrasonication. The HTCC-saponite was obtained by solution intercalation method, and then treated under ultrasonication (KQ5200B Kun Shan Ultrasonic Instruments Co., Ltd). Firstly, the equal weight ratio of HTCC and saponite were stirred at 60 °C for 24 h. Then the reaction mixture was treated under ultrasonic conditions at 60 °C for 8 h. After filtration the precipitates were washed with deionized water until no Cl^- was tested (examined by 0.1 mol/L $AgNO_3$), and then dried to yield HTCC-saponite.

Preparation of PLA/HTCC-saponite Nanocomposite. PLA, HTCC-saponite and ATBC were mixed in a high speed mixer (1000 rpm) at room temperature for 20 min, immediately after that, these mixtures were sealed for 24 h to achieve sufficient diffusion of plasticizers into PLA. The content of additional HTCC-saponite was expressed as parts per hundreds of PLA resin (phr), respectively. The mixing composition was shown in Table 1. These mixtures were manually fed into the single screw extruder (HAAKE RHEOMEX 254, diameter 19 mm and L/D =25:1, Germany) with a screw speed of 30 rpm, and the temperature profile along the extruder barrel was 170, 180, 180, and 180 °C (from feed zone to die). After these mixtures were extruded and pelletized, all samples were molded on the HAAKE MiniJet injection molding machine under a pressure of 80 MPa at 190 °C and pressure-holding time of 10 s.

Characterization. The Fourier transform infrared (FTIR) analysis of the sample was recorded by the FTIR spectrophotometer (BRUKER-EQUINOX55, Germany) using standard KBr pellet disc technique. Spectra were collected from 4000 to 400 cm^{-1} at a resolution of 4 cm^{-1}.

^{1}H NMR spectra were recorded on a VARIAN INOVA-400 spectrometer (USA) operating at 400 MHz (^{1}H). Samples were dissolved in 2% (w/w) DCl/D_2O and D_2O, respectively and introduced into a 5 mm NMR tube. The spectra were recorded at room temperature. The delay between scans was varied from 1 to 5 s in order to investigate its influence on the integral ratios.

X-ray diffraction (XRD) pattern were recorded with a Philips X'Pert X-diffractometer (Netherland), using CuKα radiation at λ=0.1540 nm (50 kV, 35 mA). Diffraction spectra were obtained over 2θ range of 1.5-60° with a scanning speed of 0.1 °/s. HTCC-saponite was studied as powders.

The morphology of HTCC-saponite and impact fracture surfaces of PLA/HTCC-saponite nanocomposites were observed by a scanning electron microscope (SEM, Inspect F, FEI Instrument Co., Ltd, Netherland) at 20 kV of acceleration voltage. Prior to SEM evaluation, the samples were sputter-coated with gold to avoid charging during the tests.

The morphology of PLA/HTCC-saponite nanocomposites was observed by a transmission electron microscope (TEM), TECNAI G2-F20 (FEI Co., Netherland). The ultracryotomy of PLA/HTCC-saponite nanocomposites samples was done by LEICA EM UC6/F6 microtome, and the thickness of ultracryotomy was about 80 nm. Specimen was observed at an acceleration voltage of 200 kV.

Thermal gravimetric analysis (TGA) was conducted on TA-Q600 analyzer (USA). Samples of about 5-10 mg were placed in an open alumina crucible. Temperature programs for dynamic were carried out at a heating rate of 10 °C/min from room temperature to 450 °C. The measurements were operated under a nitrogen purge (100 mL/min).

Differential scanning calorimetry (DSC) was conducted on a NETZSH204 DSC differential scanning calorimeter (Germany). Samples of about 5-8 mg were performed by heating from room temperature to 250 °C at a heating rate of 10 °C/min under a nitrogen flow (40 mL/min).

Crystallization was studied by polarized optical microscopy (POM) (LEICA-DMLP1, Germany). A sample was melted at 200 °C for 3 min and then rapidly cooled to a preset temperature for isothermal crystallization. The spherulites of PLA were observed in micrographs after isothermal crystallization.

Minimum inhibitory concentrations (MICs) of HTCC and chitosan against *Bacillus subtilis*, *E. coli* (*Escherichia coli*), *Aspergillus* (*Aspergillus SPP*) and *Penicillium* (*Penicillium SPP*) were determined by the approved standard method, and the bacteria were incubated at 37 °C for 24 h using Muller-Hinton Broth, respectively. Nutrient broth and tryptone glucose extract agar were bacteria cultivating reagents. Bacterial spe-

Table 1. Mixing Compositions of PLA/HTCC-saponite Nanocomposites

Compound code	Mixing composition		
	PLA (g)	ATBC (g)	HTCC-saponite (g)
PLA	150	-	-
PLA0	150	15	-
PHS1	150	15	0.45
PHS2	150	15	0.75
PHS3	150	15	1.5
PHS4	150	15	4.5
PHS5	150	15	7.5

cies (Gram-positive bacterium) was the test bacterium. The standard QB/T2591-2003 method was used to conduct antibacterial testing. It is a standard test for antibacterial activity assessment on antibacterial plastics products.

Tensile tests were carried out according to the ASTMD 412-80 standard by an Instron 4302 Universal Testing Machine (USA) at a crosshead speed of 5 mm/min. At least five measurements for each composite were performed. Sample of PLA/HTCC-saponite nanocomposites were dried in vacuum oven at 60 °C for 24 h before testing.

Notched izod impact testing was performed on a Testing Machines Inc. 43-02-01 Monitor/Impact machine according to the ASTM D256 standard. 2 mm deep notches were cut into sample beams using a TMI notch cutter. All results were presented the average values of five measurements.

Dynamic mechanical analysis (DMA) was performed in tensile mode on a DMAQ800 analyzer (USA). Temperature scans at 1 Hz frequency were carried out at a heating rate of 5 °C/min from 30 to 130 °C. Samples of PLA/HTCC-saponite nanocomposites were from the injection mold and dried in vacuum oven at 60 °C for 24 h before testing.

Results and Discussion

Chemical Composition. The chemical modification of CTS with GTMAC in the presence of water resulted in N-substitution. The FTIR spectra of CTS and HTCC are shown in Figure 2. Compared with CTS, HTCC showed characteristic peaks for GTMAC, such as the bands at 1482 and 1599 cm^{-1}, which indicated successful synthesis of HTCC. The complete disappearance of NH$_2$ band in the spectrum of water-soluble HTCC again confirmed that the epoxide in GTMAC mainly reacted with NH$_2$ groups in chitosan rather than with OH group. In addition, the spectrum showed a broad band at around 3400 cm^{-1} due to the increased number of hydroxyl groups. The reaction between the amine groups of chitosan and GTMAC was represented in Figure 1. The FTIR spectrum of HTCC is consistent with the reported result.[23,24]

The NMR spectra of the samples are shown in Figure 3. The strongest peak at δ=3.2 ppm belonged to ammonium methyl hydrogen absorption peak; the absorption peaks at δ=4.71, 2.18, 3.89, 3.71, 3.65 and 3.59 ppm belonged to H-l, H-2, H-3, H-4, H-5 and H-6, respectively; the absorption peaks at δ=4.53 and 2.71 ppm belonged to H-b and H-c, respectively. These results were consistent with the literature.[25]

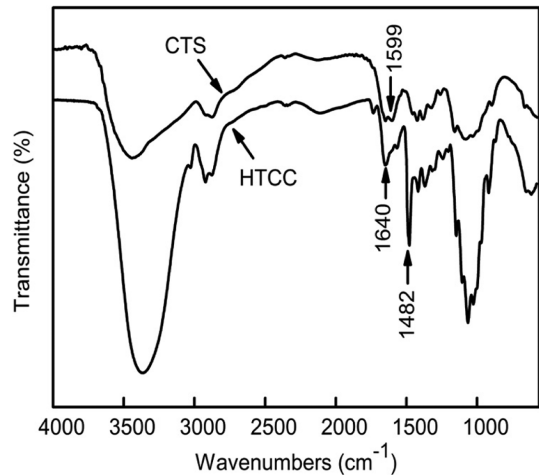As evidence of the reaction, methyl groups in the quaternary

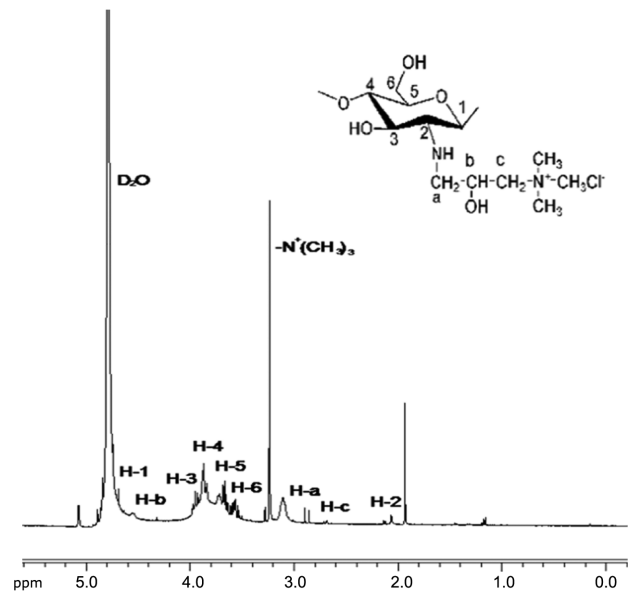**Figure 2.** FTIR spectra of CTS and HTCC.

Figure 3. ¹H NMR spectrum of HTCC.

ammonium salt group were observed as a new strong peak at 3.2 ppm in HTCC. The synthesis of HTCC is also confirmed by ¹H NMR spectroscopy.

Crystal Structure. X-ray diffraction (XRD) is a widely employed technique for the characterization of the crystalline structure of materials. Figure 4(a) shows X-ray diffraction results of HTCC-saponite and saponite. As shown in Figure 4(a), saponite had a single diffraction peak at 2θ=5.83°, corresponding to the basal reflection of (001) plane. The XRD patterns of HTCC-saponite showed that the diffraction peak (001) almost disappeared but the diffraction peak (100), (101) of HTCC were found. Compared with saponite, the intensity and area of the diffraction peak (001) of HTCC-saponite were

very weak and shifted towards smaller angle, which suggested that the layers of saponite were intercalated or partially exfoliated by HTCC. This also proved that the saponite was successfully modified.

Figure 4(b) is XRD patterns of PLA, PLA0 and PHS3 (PLA/HTCC-saponite nanocomposites). As shown in Figure 4(b), the neat PLA (PLA) exhibited two peaks at $2\theta=16.7°$ and 19.3°, which prominently indicated a crystalline PLA matrix. PLA0 had stronger characteristic diffraction peaks at ($2\theta=16.7°$, 19.3°) than that of PLA, which showed plasticization of ATBC resulted in recrystallization under the melt processing. After introduction of HTCC-saponite, the characteristic diffraction peaks (especially at $2\theta=16.7°$) of PLA based nanocomposites were stronger than that of PLA0. This phenomenon indicated that the crystallinity of PLA matrix was increased and HTCC-

saponite could be mainly responsible for this phenomenon. HTCC-saponite attached many organic cations which improved the interfacial compatibility with PLA matrix, and made HTCC-saponite evenly dispersed in PLA matrix. At the same time, nanolayers of HTCC-saponite increased the quantity of crystal nucleus and improved the heterogeneous nucleation effect. It is not hard to find from the patterns of PHS3 with 1 phr HTCC-saponite, the characteristic peaks of saponite disappeared compared with the patterns of saponite,[26] which proved that saponite had been exfoliated into nanometer scale layers by HTCC. Consequently, PLA based nanocomposites with exfoliated structure was achieved. The further confirmation of structure of saponite would be elucidated with the aid of TEM analysis.

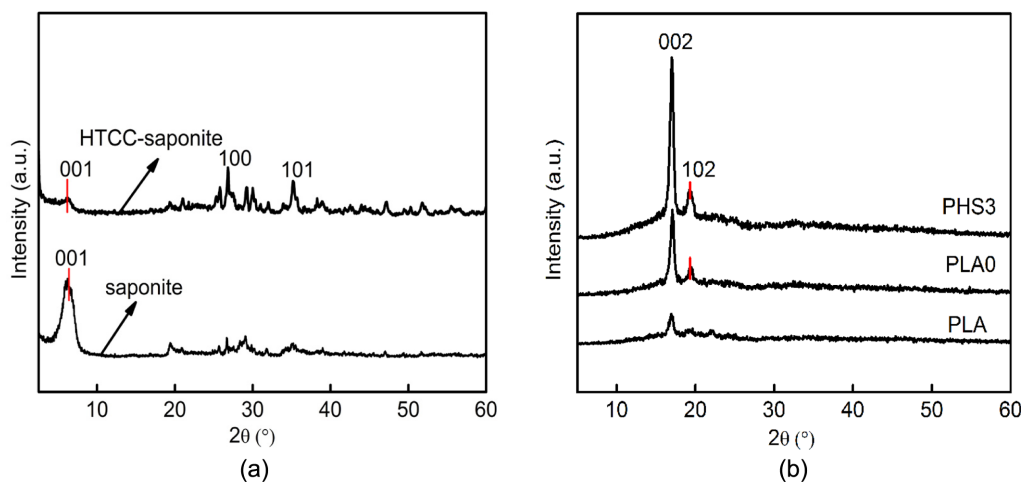**Antimicrobial Activity of HTCC.** Figure 5(a) and 5(b) are

Figure 4. XRD patterns of (a) HTCC-saponite and saponite; (b) PLA, PLA0 and PHS3.
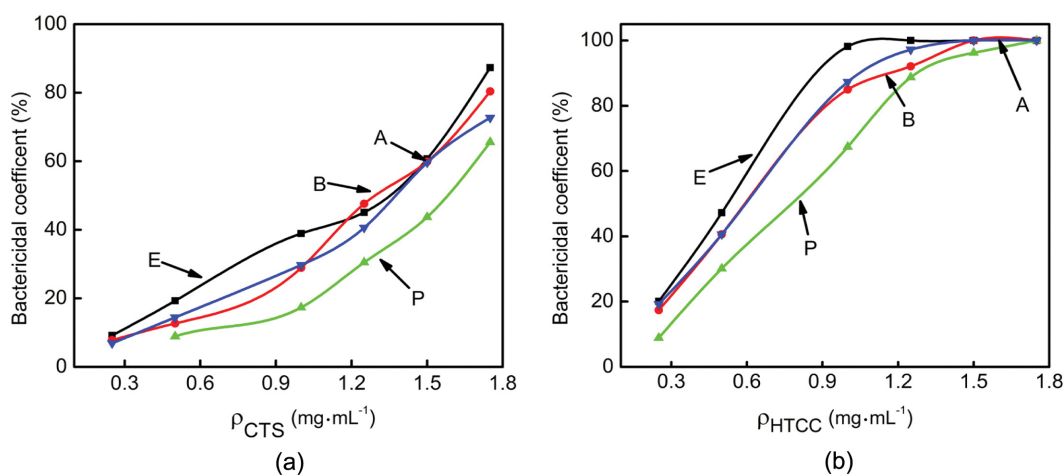

Figure 5. Antimicrobial activity of (a) CTS against (E) *E. coli*, (B) *Bacillus subtilis*, (P) *Penicillium* and (A) *Aspergillus*; (b) HTCC against (E) *E. coli*, (B) *Bacillus subtilis*, (P) *Penicillium* and (A) *Aspergillus*.

the antimicrobial activity of CTS and HTCC against (E) *E. coli*, (B) *Bacillus subtilis*, (P) *Penicillium* and (A) *Aspergillus*. The antibacterial activities of the sample were evaluated by finding the minimum inhibition concentration (MIC) as the follows: the microorganism suspension was adjusted by sterile distilled water to 10^5-10^6 cells/mL, and CTS and HTCC solutions were prepared in sterile distilled water. The resulting solutions and the nutrient agar were autoclaved at 121 °C for 20 min. Adopting double dilution method, and then the bacterial were cultured at 37 and 28 °C, respectively. MIC values were counted after cultivation of 24 h. As shown in Figure 5(a) and 5(b), with the increasing of the content of CTS and HTCC, the antibacterial ability of CTS and HTCC were stronger, respectively. By contrast, antimicrobial properties of HTCC were greatly enhanced, and with the increasing of HTCC concentration, its bacteriostatic rate was increased. Especially for *E. coli*, the MIC of HTCC reached 1 mg·mL^{-1}, so its bacteriostasis rate reached 98.2%. Compared with CTS, MIC of HTCC against these four fungi obviously increased, which showed that HTCC had good antibacterial effect. Antimicrobial properties of HTCC was mainly due to the introduction of quaternary ammonium salt groups, and the positive effect of chitosan was strengthened, which made cations enter into macromolecular polymers and combine with cell surface of the negative charged proteins, teichoic acid and lipopolysaccharide, then destroyed the permeability barrier function of cytoplasmic membrane, which led to the damage and loss of nutrients of bacteria cell, and achieved antibacterial effect;[27] or interfered with the synthesis of cell wall and dissolved the cell wall. Therefore, HTCC had strong antimicrobial properties compared with CTS.

Morphological Properties. Figure 6 was morphological images of saponite and HTCC-saponite. Figure 6(a) showed that saponite performed a uniform layer structure, and its surface was level and smooth. It was observed from Figure 6(b) that some tiny particulate matters were absorbed onto layer surface of saponite and the layer structure of saponite was intercalated. However, saponite surface in HTCC-saponite was uneven and chaotic. These phenomena demonstrated that saponite was modified by HTCC, which could be explained combined with XRD analysis of HTCC-saponite. This would be favor in improving the properties of PLA based nanocomposites. Figure 6(c) showed the stacked or agglomerated saponite layers. Figure 6(d) was TEM image of HTCC-saponite. It revealed a coexistence of intercalated or the vast majority of exfoliated layers of saponite when the content of saponite was
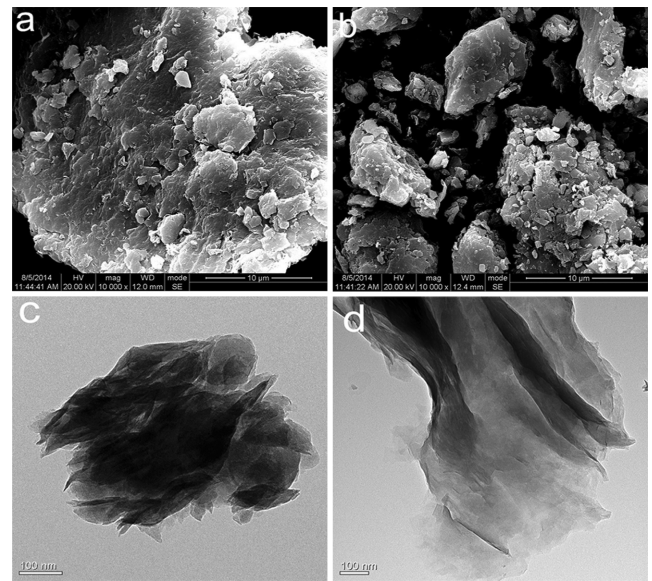

Figure 6. Morphology analysis of SEM images of (a) saponite; (b) HTCC-saponite; TEM images of (c) saponite; (d) HTCC-saponite.
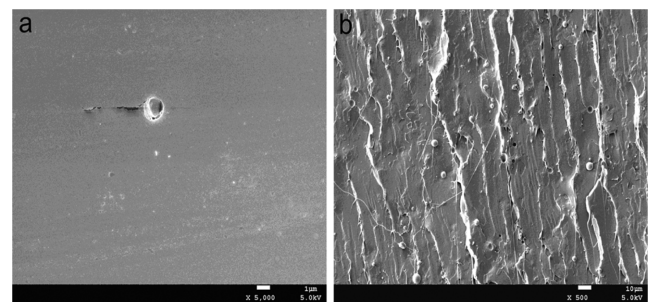

Figure 7. SEM morphologies of fracture surface of (a) PLA; (b) PHS3.

1 phr in the PLA matrix except for partial aggregation of saponite layers. Compared with saponite (Figure 6(c)), it could be clearly observed that the saponite layers in HTCC-saponite had filamentous structure, indicating that saponite was modified by HTCC. The conclusion was just as in accordance with the XRD results.

Figure 7 was the SEM images on tensile fractured surfaces of neat PLA and PHS3 (PLA/HTCC-saponite nanocomposite). From Figure 7(a), it was shown that tensile fractured surface of neat PLA was relative regular, smooth and level, which demonstrated its strong brittle fracture. However, Figure 7(b) showed PHS3 with 1 phr HTCC-saponite had multilayer, filamentous, uneven and relatively rough micrographs of fracture surface, which demonstrated that HTCC-saponite improved toughness of PLA.

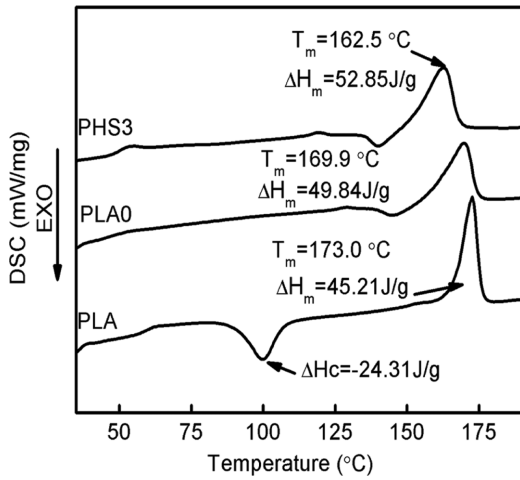**Thermal Properties.** The crystallization data of the PLA,

Figure 8. DSC curves of PLA, PLA0 and PHS3.

PLA0 and PHS3 in Figure 8 was given below:

$$X_c = \frac{\Delta H_m - \Delta H_c}{f \times \Delta H_m^o} \times 100\% \qquad (1)$$

Where, X_c=the degree of crystallinity of the PLA, ΔH_c=the enthalpy of crystallization, ΔH_m=enthalpy of fusion, f=the weight fraction of PLA in the composite, ΔH_m^o = enthalpy of fusion of the purely crystalline form of PLA (ΔH_m^o =93.7 J/g).[28] According to the above Figure 8, it was shown that T_m of PLA was 173.0 °C, and T_m of PLA0 decreased to 169.9 °C due to the plastification of ATBC for PLA. Furthermore, T_m of PHS3 significantly decreased to 162.5 °C with loading HTCC-saponite, which demonstrated HTCC-saponite also had synergia plastification because HTCC-saponite could generate hydrogen bonding with PLA and broke the intermolecular interaction of PLA. Moreover, as shown from Figure 8, the cold

crystallization of PLA disappeared after introduction of ATBC. The reason for this phenomenon was that plasticization of ATBC effectively enhanced the crystallization of PLA.[29] Figure 8 showed that the crystallinity of PHS3 was 63.37% which increased by about three-fold than that of PLA. This was in accordance with XRD analysis. This result may be attributed to HTCC-saponite which increased the crystallization of PLA with excellent nucleation effect. On the other hand, HTCC-saponite improved the interfacial compatibility between inorganic and organic phase, this contributed to reduce the activation energy of the crystallization of PLA which made the crystallization more easily and restrained the cold crystallization behavior of PLA.

Figure 9 was the results of TG-DTA analysis of PLA, PLA0 and PHS3, which were used to evaluate the thermal stability of PLA. As seen from Figure 9, it was shown that after addition of ATBC, thermal decomposition temperature (T_d) of PLA0 was 340.9 °C, which demonstrated the thermal stability of PLA was improved. Compared with PLA, when HTCC-saponite was introduced, thermal gravimetric curve of PLA based nanocomposites (PHS3) shifted to the high temperature. T_d of PLA and PHS3 were 332.5 and 351.7 °C, respectively, which showed that T_d of PLA3 was increased by 19.2 °C than that of neat PLA. So PHS3 showed good thermal stability. The main reason was that HTCC-saponite improved the thermal stability of PLA because HTCC-saponite had barrier effect towards polymer decomposition products, so the HTCC-saponite impeded the thermal motion of PLA molecular in PLA matrix, and increased the energy barrier of the thermal decomposition of PLA. Tatiana Nistor and Vasile[30] have also reported similar result.
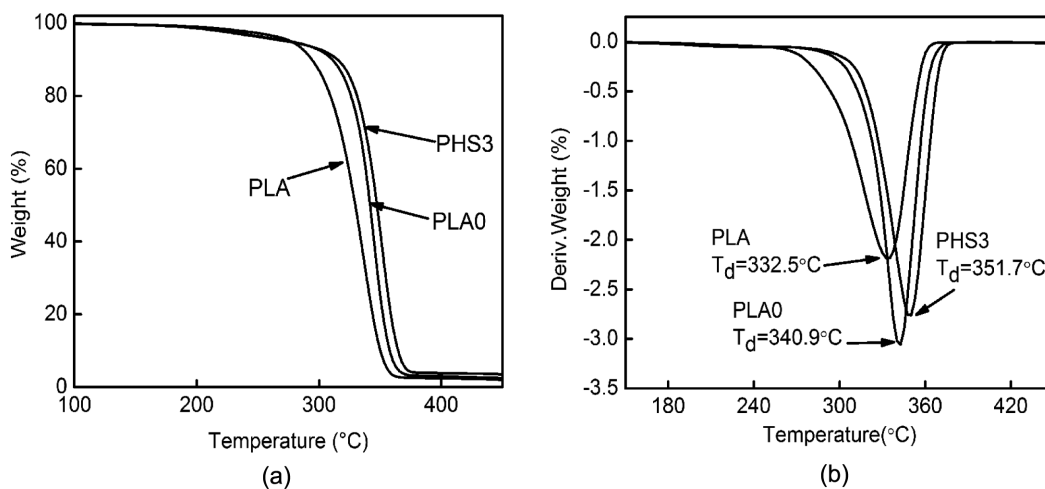

Figure 9. TG-DTG curves of PLA, PLA0 and PHS3.

Melt Crystallization Behaviors. POM was used directly to study the morphology of PLA, PLA0 and PHS3 during melt crystallization. Figure 10 represented the POM observation of neat PLA, PLA0 and PHS3 at the same moment isothermal. As seen in Figure 10, the spherulites of PLA grew hugely and collided with each other, and the grown spherulites exhibited typical extinction crosses under the polarizing microscopy, of which the diameter reached up to 50-100 μm. And the spherulite size of PLA0 was reduced to 5-10 μm or less with non-uniform distribution, which was slightly smaller than PLA due to the fact that ATBC plasticized PLA and promoted the PLA molecular chain flexibility, thus accelerated the crystallization rate. As for PHS3, very fine crystals with blurry boundaries were observed and the nucleation density was increased with introduction of HTCC-saponite. PHS3 contained the irregular sheaf-like spherulite and its numbers of spherulites were much higher than that of neat PLA and PLA0. It was clear that the nucleation density of PLA increased and the spherulite texture became finer for PLA, PLA0, PHS3, respectively. By comparing three crystalline morphologies of PLA materials sample, it was apparent that HTCC-saponite could provide the largest number of nuclei and accelerated the crystallization rate. In our work, PLA was not able to react with ATBC or HTCC-sponite, which indicated that chain scission of PLA, was not able to be caused by chemical reaction happening during the melting processing. Consequently, the nucleation mechanism of PLA induced by the chemical mechanism between PLA and ATBC and HTCC-saponite was eliminated. In view of epitaxial nucleation,[31] the polymer chains epitaxially grow on the surface of nucleating agent substrate through a physical interaction, and what is more, a good lattice matching between the two crystal structures of polymer and nucleating agent does matter. For this reason the addition of HTCC-saponite induced heterogeneous nucleation and reduced the size of the spherulites. On the other hand, the hydrogen bond interaction between PLA and HTCC-saponite might play an important role in the nucleation process.

POM analysis further confirmed that HTCC-saponite had more prominent efficiency on inducing the crystallization of PLA, which was in accord with the aforementioned DSC results.

Mechanical Properties. The mechanical properties of the neat PLA matrix and PLA/HTCC-saponite nanocomposites were listed in Table 2. Neat PLA sample and PLA/HTCC-saponite nanocomposites samples with content of HTCC-saponite of 0.3, 0.5, 1, 3, 5 phr were tested to investigate the effect of HTCC-saponite on PLA composites' elongation at break, tensile strength and impact strength. As well known, the interfacial interaction between the polymer matrix and dispersed saponite was a dominant factor in those investigated cases as demonstrated by PLA based nanocomposites.[9] As seen from Table 2, with the increasing of addition amount of HTCC-saponite, the tensile strength and elongation at break of PLA/HTCC-saponite nanocomposites were gradually increased, respectively. When the addition amount of HTCC-saponite reached 1 phr, the mechanical properties of PHS3 reached

Table 2. Mechanical Properties of PLA/HTCC-saponite Nanocomposites

Samples	Maximum tensible strength (MPa)	Elongation at break (%)	Impact strength (J/cm^2)
PLA	40.65±1.54	5.89±0.36	2.95±0.15
PLA0	45.21±1.57	6.52±0.33	3.67±0.15
PHS1	46.37±1.69	8.32±0.42	3.78±0.18
PHS2	47.61±1.73	9.35±0.48	4.11±0.21
PHS3	50.46±1.82	12.09±0.61	5.23±0.26
PHS4	46.75±1.61	11.01±0.55	4.32±0.22
PHS5	40.57±1.51	8.74±0.44	3.73±0.19

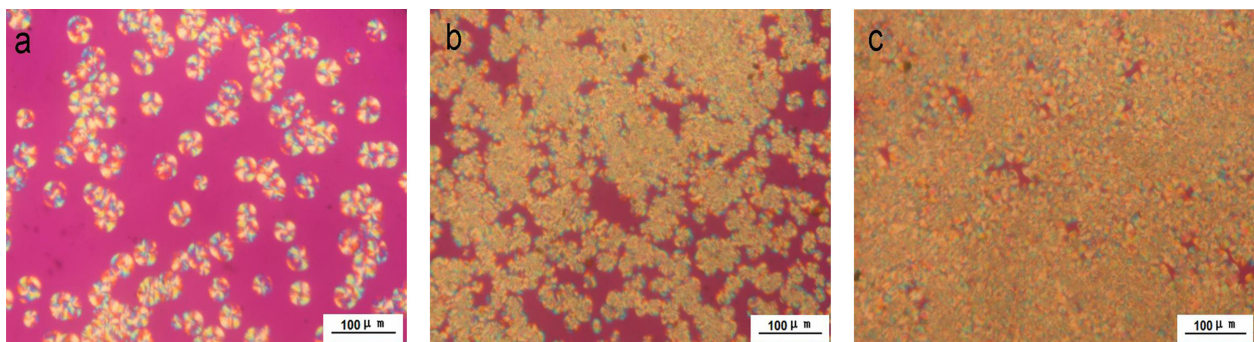**Figure 10.** POM images for (a) PLA; (b) PLA0; (c) PHS3 isothermally crystallized at 130 °C for 15 min.

maximum. Especially, only this particular PHS3 had a lower modulus and exhibited significant stress-whitening and necking behavior with a large extension, elongation at break being increased to 12.1%, which was up to 1.8-fold increment compared to the neat PLA. This is mainly because HTCC-saponite and PLA matrix has good interfacial compatibility, so HTCC-saponite nanoparticles had good reinforcement effect and certain toughening effect on PLA. When the addition amount of HTCC-saponite was more than 1 phr, tensile strength and elongation at break of PLA/HTCC-saponite nanocomposites clearly decreased, which showed when the addition amount of HTCC-saponite was too high, HTCC-saponite nanoparticles aggregated and the dispersion of HTCC-saponite in the PLA matrix became poor, which resulted in that the mechanical properties of PLA/HTCC-saponite nanocomposites decreased. The current results suggested that dispersion status and interfacial interaction were the important factors in attaining the optimum performance of PLA based nanocomposites in terms of tensile properties here.

The impact strength is the characterization of resistance to high pressure caused by rupture of ability, direct relationship between the material toughness.[32] The notched izod impact strength of the neat PLA showed impact strength of 2.95 J/cm^2, which indicated a very brittle polymer. In the PLA/HTCC-saponite nanocomposites system, it was found that when the 1 phr of HTCC-saponite was added into the PLA, the impact strength of PHS3 increased significantly from 2.95 to 5.23 J/cm^2, which demonstrated HTCC-saponite improved toughness of PLA. Consequently, the mechanical properties results were in accordance with the analysis of SEM images on tensile fractured surfaces.

Dynamic Mechanical Properties. The temperature curves storage (elastic) modulus and loss factor (tan δ) of PLA were shown in Figure 11(a), which showed that the storage modulus of the composites was higher than that of PLA matrix, due to the reinforcement effect imparted by the HTCC-saponite. The storage modulus decreased with the increase of temperature in the cases of all samples, and there was a significant fall in the regions between 50 and 80 °C. It was easy to find PHS3 had the longer plateau on the storage modulus than that of neat PLA where the softening temperature was increased from about 40 to 60 °C, which implied an increase in thermal stability of the neat PLA matrix with the addition of HTCC-saponite, and it was further increased when the PLA based nanocomposite was crystallized.[33,34] Figure 11(b) showed tan δ of PLA, PLA0 and PHS3 was as a function of temperature, where the ratio of storage modulus and loss modulus gave the tangent of the phase angle delta, a measure of energy dissipation. Loss factor in the transition region measured the imperfections in the elasticity of a polymer, with the possibility of additional losses occurring at the matrix interface.[35] As seen in Figure 11(b), HTCC-saponite contribution to the damping was low compared to that of PLA matrix. This suggested that the combined attenuation of PLA/HTCC-saponite nanocomposites would be mainly caused by the molecular motion of PLA and the interfacial interaction of the HTCC-saponite.

Figure 11(b) also showed that a lot of alterations were also recorded in tan δ curves. T_g of PLA was found at 69.35 °C, while T_g of PLA0 shifted to slightly higher values. As for PHS3, its T_g increased to 80.33 °C with the addition of HTCC-
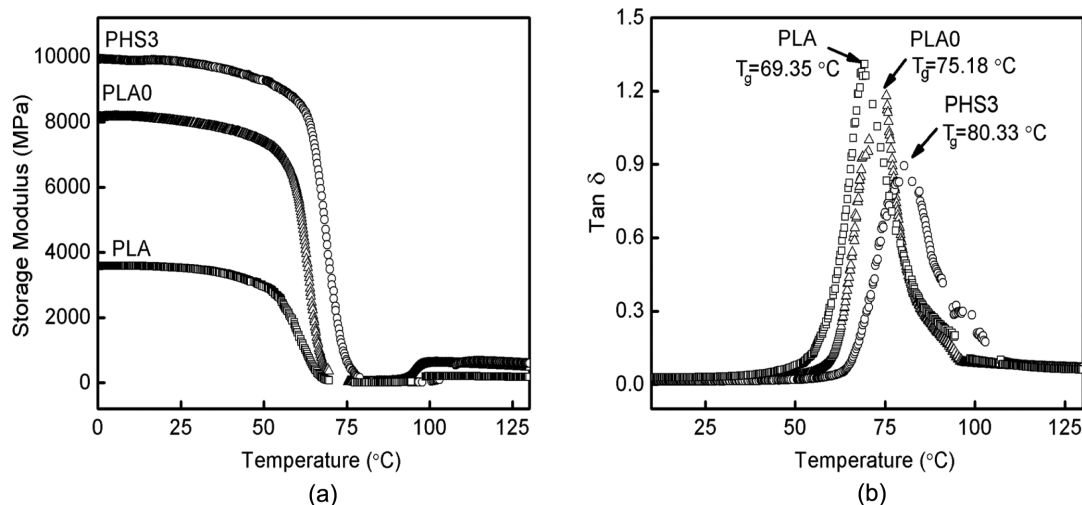

Figure 11. Temperature dependence of (a) storage modulus; (b) tan δ.

saponite, due to the interactions between the PLA chains and HTCC-saponite layers and the reduction of macromolecular chain mobility at the zone surrounding the nanoparticles. This was clearer compared with the peak areas of neat PLA and PHS3, which was drastically decreased after the addition of HTCC-saponite nanoparticles. T_g was a complex phenomenon depending on a number of factors such as chain flexibility, molecular weight, branching, cross-linking, intermolecular interactions and steric effects. The increase of T_g (11 °C) after the addition of HTCC-saponite could be attributed to the decrease in free volume in the PLA matrix due to the physical cross-linking caused by the interactions between the organic groups of HTCC-saponite and PLA.[36] However, it seemed that the chain segment mobility of the PLA phase was drastically influenced by the introduction of HTCC-saponite.

Conclusions

HTCC was prepared with 2, 3-epoxypropyl trimethyl ammonium chloride grafting to the amino groups of chitosan. Then, HTCC-saponite was synthesized with HTCC and saponite under ultrasonication intercalation. Compared with chitosan, MIC of HTCC against these four fungi obviously increased, which showed that HTCC had good antibacterial effect. To improve the crystallization and comprehensive properties of PLA, a series of thermoplastic PLA/HTCC-saponite nanocomposites were successfully prepared by melting processing. It was shown that HTCC-saponite was exfoliated into nanoscale layers and performed as a heterogeneous nucleation effect in PLA matrix, which accelerated the crystallization of PLA. At the same time the comprehensive performance of PLA based nanocopmposites were significantly enhanced.

References

1. E. Nieddu, L. Mazzucco, and P. Gentile, *React. Funct. Polym.*, **69**, 371 (2009).
2. S. S. Ray, K. Yamada, and M. Okamoto, *Macromol. Mater. Eng.*, **288**, 203 (2003).
3. M. Pluta, A. Galeski, M. Alexandre, M. A. Paul, and P. Dubois, *J. Appl. Polym. Sci.*, **86**, 1497 (2002).
4. J. Y. Nam, M. Okamoto, H. Okamoto, M. Nakano, A. Usuki, and M. Matsuda, *Polymer*, **47**, 1340 (2006).
5. R. Auras, B. Harte, and S. Selke, *Macromol. Biosci.*, **4**, 835 (2004).
6. W. Y. Jang, K. H. Hong, B. H. Cho, S. H. Jang, S. I. Lee, and B. S. Kim, *Polym. Korea*, **32**, 116 (2008).
7. S. H. Lee, D. Kim, J. H. Kim, D. H. Lee, S. J. Sim, J. D. Nam, H. Kye, and Y. K. Lee, *Polym. Korea*, **28**, 519 (2004).
8. M. A. Paul, M. Alexandre, C. Henrist, A. Rulmont, and P. Dubois, *Polymer*, **44**, 443 (2003).
9. W. J. Zhen and J. L. Sun, *Polym. Korea*, **38**, 299 (2014).
10. G. Z. Papageorgiou, D. S. Achilias, S. Nanaki, T. Beslikas, and D. Bikiaris, *Thermochim. Acta*, **511**, 129 (2010).
11. W. J. Zhen, C. H. Lu, C. Y. Li, and M. Liang, *Appl. Clay Sci.*, **57**, 64 (2012).
12. S. Morfis, C. Philippopoulos, and N. Papayannakos, *Appl. Clay Sci.*, **13**, 203 (1998).
13. J. Hrobarikova, J. L. Robert, and C. Calberg, *Langmuir*, **20**, 9828 (2004).
14. M. N. Ravi Kumar, *React. Funct. Polym.*, **46**, 1 (2000).
15. Z. Zhong, X. Ji, and R. Xing, *Bioorg. Med. Chem.*, **15**, 3775 (2007).
16. S. H. Lim and S. M. Hudson, *Carbohydr. Res.*, **339**, 313 (2004).
17. C. H. Kim, J. W. Choi, H. J. Chun, and K. S. Choi, *Polym. Bulletin*, **38**, 387 (1997).
18. M. Ma, H. S. Zhang, L. Y. Xiao, L. Xiao, P. Wang, H. R. Cui, and H. Wang, *Electrophoresis*, **28**, 4091 (2007).
19. Q. X. Ji, X. G. Chen, and Q. S. Zhao, *J. Mater. Sci. - Mater. Med.*, **20**, 1603 (2009).
20. C. Q. Qin, Q. Xiao, H. R. Li, M. Fang, Y. Liu, X. Chen, and Q. Li, *Int. J. Biol. Macromol.*, **34**, 121 (2004).
21. A. F. Kotzé, M. M. Thanou, H. L. Luessen, and H. E. Junginger, *Eur. J. Pharm. Biopharmaceut.*, **47**, 269 (1999).
22. H. Li, Y. Du, X. Wu, and H. Zhan, *Colloids Surf., A*, **242**, 1 (2004).
23. Y. H. Kim, J. W. Choi, and E. Y. Lee, *Polym. Korea*, **27**, 405 (2003).
24. Q. C. Qin, X. Ling, D. Yumin, S. Xiaowen, and C. J. Wei, *React. Funct. Polym.*, **50**, 165 (2002).
25. M. J. Zohuriaan-Mehr, *Iranian Polym. J.*, **14**, 235 (2005).
26. X. Mao, W. Zhen, and L. Wang, *Plast. Sci. Technol.*, **39**, 86 (2011).
27. S. H. Lim and S. M. Hudson, *J. Macromol. Sci., Part C: Polym. Rev.*, **43**, 223 (2003).
28. D. Garlotta, *J. Polym. Environ.*, **9**, 63 (2001).
29. H. Bai, H. Xiu, and J. Gao, *ACS Appl. Mater. Inter.*, **4**, 897 (2012).
30. M. T. Nistor and C. Vasile, *Iranian Polym. J.*, **22**, 519 (2013).
31. P. Song, G. Y. Chen, Z. Y. Wei, Y. Chang, W. X. Zhang, and J. C. Liang, *Polymer*, **53**, 4300 (2012).
32. C. S. Yoon and D. S. Ji, *Polym. Korea*, **33**, 581 (2009).
33. P. S. Chua, *Polym. Compos.*, **8**, 308 (1987).
34. K. Choi, H. S. Lee, and B. C. Kang, *Polym. Korea*, **34**, 294 (2010).
35. S. K. Majhi, S. K. Nayak, S. Mohanty, and L. Unnikrishnan, *Int. J. Plast. Technol.*, **14**, 57 (2010).
36. S. S. Ray, K. Yamada, M. Okamoto, and K. Ueda, *Polymer*, **44**, 857 (2003).